18th Brazilian Congress of Thermal Sciences and Engineering
November 16-20, 2020 (Online)

ENC-2020-0669
DEVELOPMENT OF A MATHEMATICAL MODEL FOR THE EVALUATION OF UNGLAZED SOLAR COLLECTORS

Marcus Vinicius Braga Bazzoni
Roan Borges de Thuin
Tassia Luiza Ferreira Morais
Cristiana Brasil Maia
Lucas Paglioni Pataro Faria
Pontifícia Universidade Católica de Minas Gerais, Av. Dom José Gaspar, 500 Coração Eucarístico – Belo Horizonte MG 30535-901
E-mails: marcusbazzoni@hotmail.com, roanthuin@hotmail.com, tassia.fmorais@gmail.com, cristiana@pucminas.br, lucas.faria@pucminas.br

Abstract *This paper presents a mathematical model of an unglazed solar collector. The model was developed using Excel VBA and it allows the prediction of the temperature profile of the water along the tube and the system efficiency. The mathematical model was simulated assuming similar behavior in the tubes. The analysis was performed considering a different number of elements along the tube, for different mass flow rates. The results of the simplified model indicated that the prediction of the thermal performance was as expected, allowing to state that the model is a valuable tool for fast and reliable collector simulation. The results were compared with experimental data seeking a validation.*
Keywords: *Unglazed solar collector, Mathematical modelling, Thermal performance*

1. INTRODUCTION

Over the last years, the demand for clean and renewable energy increased with the rising of environmental concern regarding global warming. Under these circumstances, solar energy became one of the most abundant and sustainable sources, being known by its versatility. It has numerous applications in the industrial and domestic sector, such as space heating, and swimming pool heating.

Swimming pool heating systems use solar collectors as an instrument for the conversion of solar radiation from the sun into heat to warm the water contained in the pool. There are two major classes of solar collector, they are differentiated by the presence or absence of a glaze or cover. Glazed solar collectors have various design parameters, number, type, and thickness of glaze, type of coating on the absorber plate, and spacing between the absorber and the inner glass, to name a few. Unglazed solar collectors do not have this many design parameters and can deliver a higher solar energy efficiency at temperatures near to the ambient (M. Bunea et al., 2015).

In order to shorten the costs of production, new materials are used in this kind of collectors that are more environmentally friendly and do not interfere negatively on its efficiency, such as polymers (Missirlis et al., 2014). Recent researchers adopted this material by its important characteristics, low cost, and corrosion resistance. Polymeric solar collectors are broadly spread, mostly applied as reduced cost and unglazed swimming pool heaters (Alghoul et al., 2005).

In 2017, unglazed solar collectors had a share of 6.1% of the total of collectors installed in operation worldwide, and Brazil is the third country with higher cumulated water collector installations of this type, only behind United States of America and Australia (IEA, 2019).

Unglazed solar collectors are vastly used and had been adopted by many countries, nevertheless there is no procedure of quantifying its performance that is largely acknowledged (Morrison et al., 1992). The parameters capable of affecting its performance are the amount of incident solar radiation, the ambient and inlet temperature, the mass flow rate of the fluid, among others. Recent work (D. Missirlis et al., 2014) studied the influence of different manifold configurations on the heat transfer behavior of a polymer solar collector with a computational fluid dynamics (CFD) model. Another research (M. Bunea et al., 2015) developed a mathematical model for a solar collector considering the condensation and frost effect, rain heat gains or losses, wind speed and long wave irradiation. Recently, Cunio and Sproul (2012) investigated the theoretical and experimental performance of uncovered swimming pool solar collectors under reduced flow rate conditions.

To carry an accurate performance analysis a mathematical model can be developed. It can improve the precision and speed of calculation and reduce the validation process time. The purpose of this paper is to develop a mathematical model to evaluate and investigate the expected theoretical performance of an unglazed polymeric solar collector. VBA (Visual Basic for Applications) was used to conduct the model.

2. THEORETICAL MODELLING

Models for solar collectors have existed in the past and due to the success of Duffie and Beckman in the subject their model was chosen as guide. Figure 1 corresponds to the re-interpretation of the problem, using Whillier (1953, 1977) and Hottel and Whillier (1958) as guide. Since the collector has no 1st or 2nd cover and no absorber plate as the author suggests (no true scale was represented) the following is the result:

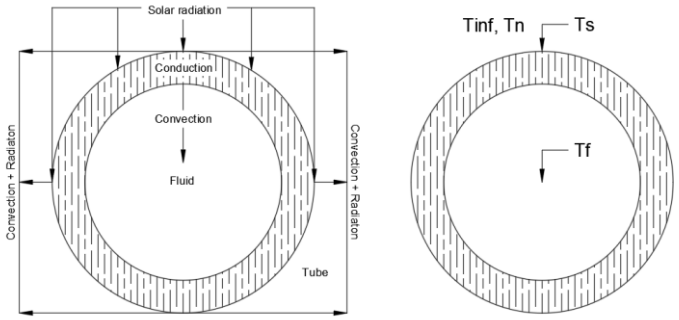

Figure 1. Two cross-sections from one of the parallel tubes of the with the heat flux scheme and one with temperatures.

It should be said that the area of incidence of the solar radiation, heat loss from convection and radiation are different. The solar radiation, as seen in the figure 1, uses the half top of the surface area of the tube, as the other ones uses all of it. Several factors still must be considered like the difference between the half top and bottom for all heat losses due to difference in the environment itself, but before going any further some assumption have had to been made, Duffie (2013):

1. Performance is steady state.
2. Construction is of sheet and parallel tube type.
3. The headers cover a small area of collector and can be neglected.
4. The headers provide uniform flow to tubes.
5. There is no absorption of solar energy by a cover insofar as it affects losses from the collector.
6. The sky can be considered as a blackbody for long-wavelength radiation at an equivalent sky temperature.
7. Temperature gradients around tubes can be neglected.
   The temperature gradients in the direction of flow and between the tubes can be treated independently.
8. Properties are independent of temperature.
9. Dust and dirt on the collector are negligible.

Based on that, a simple energy balance was elaborated, but first, it is important to mention that the area used is a function of the length of the tube demonstrated below:

$$A = \pi \times D \times L \tag{1}$$

$$A_e = \frac{A}{L} \text{ and } A_i = \frac{A}{L} \tag{2}$$

where A is the area of the surface (m²) A_i and A_e are the internal and external areas as a function of the length (m²/m) to make the model more suitable for the simulation.

The complete energy balance is defined together with the thermal resistance's circuit in Fig. 2:

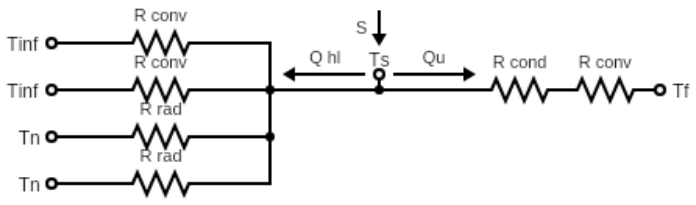

Figure 2. Thermal resistances scheme

$$S = Q_u + Q_{conv} + Q_{rad} \tag{3}$$

Where S is the heat absorbed by the tube (W/m), Q_U is the useful heat that goes into the fluid (W/m), Q_{conv} is the heat change due convection (W/m) and Q_{rad} is in relation to radiation (W/m).

In the following all the heat equations will be defined beginning with solar radiation heat:

$$S = q" \times \frac{1}{2} \times Ae \tag{4}$$

Where $q"$ is solar heat flux, Ae is the external and area (m²/m), in the sequence, convection heat:

$$Q_{conv} = h_e \times Ae\ (T_s - T_\infty) \tag{5}$$

The parameter T_∞ is the environmental temperature, T_s is the surface temperature of the tube (K), h_e is the convection coefficient from external surfaces.

$$Q_{rad} = \varepsilon \times Ae \times \sigma \times \left({T_s}^4 - {T_n}^4\right) \tag{6}$$

T_s , T_∞ ,T_n and T_f are surface (of the tube), ambient, neighborhood and fluid temperatures (K), ε is emittance (-), σ is the Stefan-Boltzmann constant (W/m² K^{-4}).

$$Q_U = \frac{1}{R_{conv}+R_{cond}} \times \left(T_s - T_f\right) \tag{7}$$

With R_{conv} and R_{cond} defined by:

$$R_{cond} = \frac{\ln\frac{De}{Di}}{2 \times \pi \times k} \qquad \text{and} \qquad R_{conv} = \left(\frac{1}{h_i \times A_i}\right) \tag{8}$$

Where De and Di are the external and internal diameters (m), k is the conductive constant (W/m). And Q_U can be rewritten as:

$$Q_U = \frac{1}{R_{CC}} \times \left(T_s - T_f\right) \tag{9}$$

With R_{CC} being the sum of R_{cond} with R_{conv}.

The next step was to get equations 4,5,6,7, and substitute in equation 3. In the resulting equation, it was able to verify that two variables are undetermined: T_S for the surface temperature and T_f for the fluid temperature, these variables vary with the length of the tube. Once T_f for L = 0 was assumed as the same as the inlet temperature of the system, then it is possible to calculate the T_S for L = 0 To solve the equation though it was easier to isolate T_S existent in the first term at the right side of the equation, propose a reasonable T_S to start with and let it converge to the answer substituting the calculated one as new input. After testing it, few iterations and equation 9 was sufficient to achieve the precision it required:

$$T_s = R_{CC} \times (S - Q_{rad} - Q_{conv}) + T_f \tag{10}$$

With the surface temperature T_s for the initial length now calculated, it was possible to calculate Q_u using the equation number 3. Attributing T_s value as constant for a small length, dL, the variation of temperature could be calculated using the following formulas:

$$Q_u = \dot{m} \times cp \times \left(T_{f_{L+d_L}} - T_{f_L}\right) \tag{11}$$

$$T_{f_{L+d_L}} = \frac{Q_u}{\dot{m} \times cp} + T_{f_L} \tag{12}$$

where $\dot{m}$ is the mass flow rate (kg/s), cp is the specific heat (J/kgK) and the temperatures $T_{f_{L+d_L}}$ and T_{f_L} (K) are the fluid temperatures in the section d_L as shown in the figure below, at the left we have a section of the tube and temperatures corresponding to the faces in which they are draw in the left of the section T_{f_L} and in the right $T_{f_{L+d_L}}$, it is worth it to mention that the smaller the d_L, the closer to the reality the model is.

The figure has no scale and only serve a purpose of better visualization:

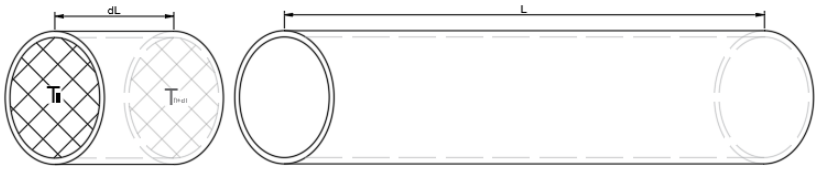

Figure 3. Scheme of a collector tube

At this point, $T_{f_{L+d_L}}$ was attributed as T_{f_L} for the next element of length d_L until their sum cover the entire length of the original tube.

Assuming that the flow inside all the tubes is uniform, the efficiency of one tube is the same as the collector, but the heat absorbed by the collector is the Q_{uT} multiplied by the numbers of tubes.

$$Q_{u_T} = \sum_{i=0}^{n_e}\left(Q_{u_i} \times d_{L_i}\right) \tag{13}$$

$$Q_c = Q_{u_T} \times n_t \tag{14}$$

With Q_{u_T} as the whole heat absorbed by the fluid in one tube (W), n_e is the number of elements, Q_c is the heat absorbed by the collector (W) and n_t is the number of tubes on the collector.

The efficiency is the whole heat absorbed by the fluid in one tube (Q_{u_T}), over the whole solar radiation in one tube.

$$\eta = \frac{Q_{u_T}}{S \times L} \times 100\% \tag{15}$$

To calculate the convective coefficient for internal fluid flow in a circular tube it was used the expression (Cengel, 2002):

$$h_f = \frac{N_u k}{D_i} \tag{16}$$

With N_u as the Nusselt number, k as the thermal conductivity of the fluid and D_i as the internal diameter of the tube. To calculate the Nusselt number, it is important that first the Reynolds number is known. When $Re < 2300$, the flow is laminar, and Nusselt is between the range of 3.66, for constant temperature along the pipe and 4.36, for constant heat flux (Cengel and Cimbala, 2006). When analyzing a plastic solar collector with laminar flow, the constant heat flux reference is more appropriate (Cunio and Sproul, 2012).

Nusselt can assume other values when the flow is transitional or turbulent ($2300 < Re < 10000$), and can be calculated with the equation (Cengel and Cimbala, 2006):

$$N_u = \frac{(f/8)(Re-1000)Pr}{1+12.7(f/8)^{0.5}(Pr^{2/3}-1)} \tag{17}$$

With N_u as the Nusselt number, Pr as the Prandt number, Re as the Reynolds number and f as the Darcy Friction factor.

And lastly, when the flow is turbulent ($Re > 10000$), Nusselt can be reached with another expression (Incropera, 2010):

$$N_u = 0.027 Re^{4/5} Pr^{1/3} \left(\mu/\mu_s\right)^{0.14} \tag{18}$$

With N_u as the Nusselt number, Pr as the Prandt number, Re as the Reynolds number, and considering the last term, the relation of viscosities, equal to 1. This approximation is possible assuming that these values do not vary with the temperature.

The Reynolds is given by:

$$Re = \frac{\rho V D}{\mu} \tag{19}$$

Where μ is the viscosity of the fluid (Ns/m^2), ρ is the density (kg/m^3) and V the flow velocity (m/s).

The external convection coefficient can be calculated with a correlation using linear function introduced in 1981 (Test et al., 1981), where the coefficients of the equation are experimentally defined. The linear function has the generic form:

$$h_e = A + BV \tag{20}$$

Following Cunio et al. considerations, the coefficient A assumes the value of 4.1 (Australian Standards, 1989), and B the value of 8.3 (Sharples and Charlesworth, 1997). Both coefficients are suitable for unglazed solar collectors instead of flat plate collectors. Thus, the convective coefficient adopted by this study has the form:

$$h_e = 8.3 + 4.1V \tag{21}$$

With h_e as the external convective heat transfer coefficient and V as the wind velocity.

3. MATHEMATICAL MODELLING

One of the most important characteristics of a solar collector is its efficiency. Towards this direction, the mathematical model was developed using the previously mentioned theoretical considerations to ascertain the collector efficiency, its temperature variation, temperature profile, total collector heat absorbed and processing time.

The model was developed using the Excel VBA (Visual Basic for Application) and it is summarized in the Fig. 4 and needs some input parameters to work. These parameters refer to the collector's characteristics and its environment.

In order to observe the influence of the number of elements considered in one tube and also to observe the behaviour with different mas flow rates it was executed different simulations varying number of elements and mass flow from all the input parameters. The dimensions input parameters were based on an existent swimming pool collector, the values of convection coefficients were estimated, the physical properties of Polypropylene were given by (Antonella Patti and Domenico Acierno, 2019) and those are shown below.

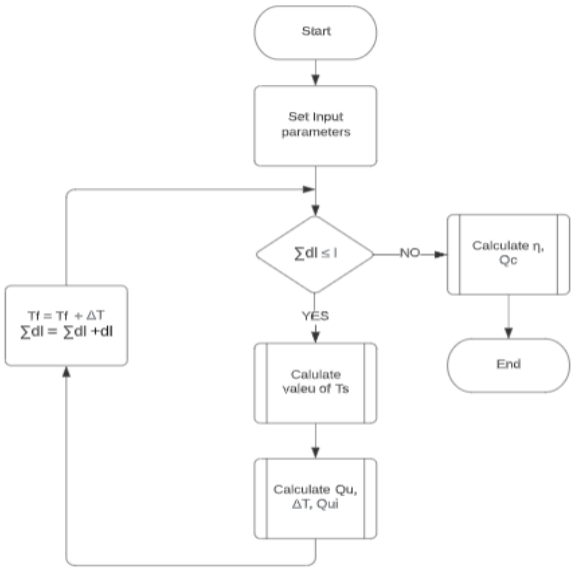

Figure 4. Calculus flow chart.

They are:

- Q_v Volumetric flow of the system in litres/minute. Varies.
- C_p Specific heat of the water at the inlet temperature.
- ρ Density of the water at inlet temperature.
- μ Dynamic viscosity of the water at inlet temperature.
- Pr Prandt value of the water at the inlet temperature.
- $k_{água}$ Conduction coefficient of the water at the inlet temperature.
- d_i Inner diameter of the tube in m. $d_i = 0.0085$ m
- d_e External diameter of the tube in m. $d_e = 0.0065$ m
- ε Emittance of Polypropylene. (Patti, A. and Acierno, D.) $\varepsilon = 0.97$
- R_a Roughness of polypropylene (Patti, A. and Acierno, D.) $R_a = 2 * 10^{-5}$
- k Conduction coefficient of polypropylene in W/ (m K) k = 0.22 W/ (m k)
- n Number of tubes on collector. n = 85
- q" Solar heat flux in W/m^2 q" = 815 W/m^2
- T_0 Inlet water temperature K. $T_0 = 296.80$ K

- $T_{infBottom}$ Environment bottom temperature in K. $T_{infBottom}$ = 296.04 K
- $T_{nBottom}$ Surrounding bottom temperature in K. $T_{nBottom}$ = 286.52 K
- T_{infTop} Environment top temperature in K. T_{infTop} = 296.04 K
- T_{nTop} Surrounding top temperature in K. T_{nTop} = 286.52 K
- l Length of the tube. l = 1.935
- n_e Number of elements considered on tube. Varies.

3.1 Influence of Volumetric and therefore mass flow

To observe the influence of volumetric flow in the system, which is directly proportional to the mass flow, once mass flow equals volumetric flow times density, it was executed the program four times with 1935 number of elements and varying the mass flow as shown in Tab. 1.

Table 1. Results varying mass flow

Total Mass Flow	ΔT	Collector Efficiency	Total Collector Heat absorbed
0.120 l/min	16.5K	7.67%	137 W
0.600 l/min	13.9 K	32.5%	582 W
6.00 l/min	2.80 K	65.3%	1.17E3 W
60.0 l/min	0.317 K	73.79%	1.32E3 W

The Fig. 5 shows the temperature profile along the tube for these simulations.

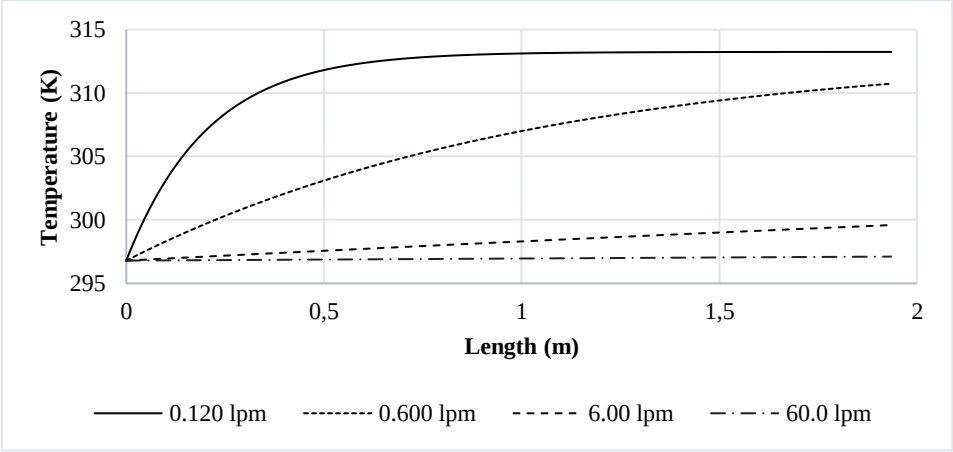

Figure 5. Temperature profile along the tube, varying the volumetric flow

It is possible to observe on the Tab. 1 two big differences, as the volumetric flow increases, the efficiency also increase, but the variation of temperature decreases.

The reason for the fact that the variation of temperature decreases is related with the Eq. (11), since the mass flow have increased, to maintain the same value of Q_u the variation of temperature must decrease for that element and that is the reason for the growth of efficiency values, once the variation of temperature is now smaller, the efficiency of each element varies less and then keeping the result higher along the tube.

Analysing the Fig. 5, the lower the mass flow, the higer the variation of efficiency on each element along the tube and more the temperature profile tends to the logarithimic behaviour. Also the higher the mass flow, the lower the variation of efficiency on each element, therefore the behaviour of temperature profile tends to a linear function. This statement is visible on Fig. 5 with the flow as 0.120 lpm the curve tends to the logarithimc function, for flow as 0.600 lpm it is possible to observe a slightly curvature on temperature profile, for flow as 6.00 lpm, the temperature profile tends to a linear function and for mass flow as 60.0 lpm it did not have any significative variation of temperature.

3.2 Influence of number of elements, low volumetric flow rate.

With the purpose to observe the influence of number of elements along the tube, it was executed the program five times, all those five simulations had the same mass flow, but the number of elements varying as shown in Tab. 2.

The value of mass flow was chosen in order to make the results more visual, contributing to the analysis of results.

Table 2. Results varying number of elements with volumetric flow rate of 0.120 lpm.

Number of Elements	ΔT	Collector Efficiency	Total Collector Heat absorbed	Processing Time
1	153 K	71.4%	1.28E3 W	0.0781 s
10	16.5 K	7.67%	137 W	0.207 s
300	16.5 K	7.67%	137 W	1.90 s
1935	16.5 K	7.67%	137 W	13.1 s

The Fig. 6 show the temperature profile of the water and the surface along the tube of the simulations, excluding the first one, because analysing its result was considered impossible.

Once the Q_u was considered constant all along the tube, the temperature of water, T_f, at the end of tube was higher than the surface temperature T_s. According to the Thermodynamics laws, the heat flows from the higher temperature to the lower temperature, and as known, the tube surface absorbs the heat from solar radiation, in this case, its temperature must be higher than what is inside.

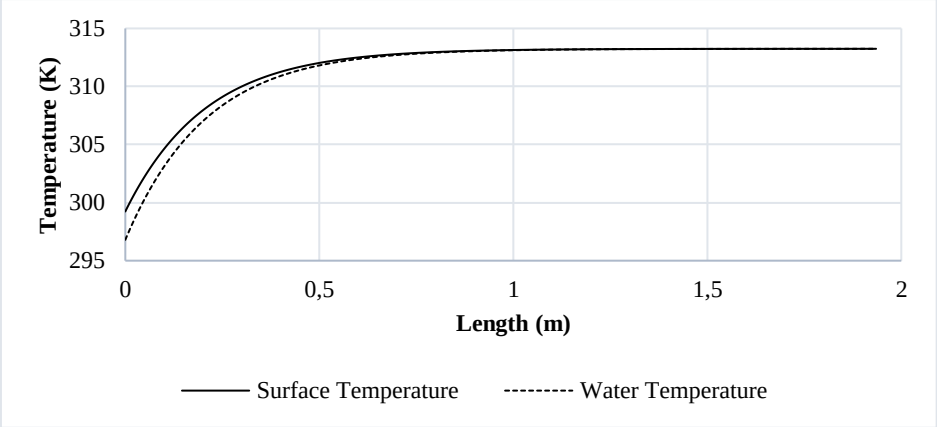

Figure 6. Temperature profile for the simulations.

The results on Fig. 6 are as expected, with a logarithmic behaviour and T_f tending to T_s and always below, because analysing the Eq. (5), (6) and (10) it is possible to see that for Q_{conv} and Q_{rad} that , T_∞ and T_n stays the same for all the tube and T_s increases. Therefore, Q_{conv} and Q_{rad} both increase and due to this, as shown on energy balance on Eq. (10), Q_u decreases until it is negligible, with Q_u negligible, with the Eq. (11), the variation of temperature from one element to other is also negligible.

Analysing the results on Tab. 2, it is possible to see that the Collector efficiency, and therefore the temperature variation, Total Collector Heat absorbed vary with the number of elements. This variation occurs since increasing the number of elements, Q_u is attributed for smaller lengths and is calculated more precise values of Q_u.

It is also possible to observe that there is no variation between the efficiency of 10 elements and 300 elements and between 300 and 1935 for this situation, but the processing time increases significantly with the number of elements, therefore, depending on the situation, it will not make difference to run the program with a large number of elements. It is important to emphasise that those results were for these input parameters and it should change if there were different input parameters.

3.3 Influence of number of elements, high volumetric flow rate.

Table 3. Results varying number of elements with volumetric flow rate as 12.0 l/min

Number of Elements	ΔT	Collector Efficiency	Total Collector Heat absorbed	Processing Time
1	1.53 K	71.4%	1.28E3 W	0.0703 s
10	1.47 K	68.5%	1.23E3 W	0.215 s
300	1.46 K	68.3%	1.22E3 W	1.87 s
1935	1,46 K	68.2%	1.22E3 W	10.8 s

For this input parameters the same behaviour of variation of efficiency from smaller values of n_e to biger values was noticed, the variation between 10 to 300 was 0.2% while between 300 to 1935 was 0.1%.

It is possible to see that for this input parameter the values from 1 element was closer than in section 3.2, the reason for this is related to a combination of d_L and mass flow, the higher the mass flow, the higher d_L can be, because local efficiency varies less as a function of length, so it is reasonable to assign a constant value of Q_U for a larger stretch and smaller values of n_e are required, but if the mass flow is small, local efficiency has greater variations as a function of length, requiring smaller values of dl, therefore, higher values of n_e are required.

With the local efficiency varying less as a function of length it is possible to observe that the temperature profile tends to a linear behaviour.

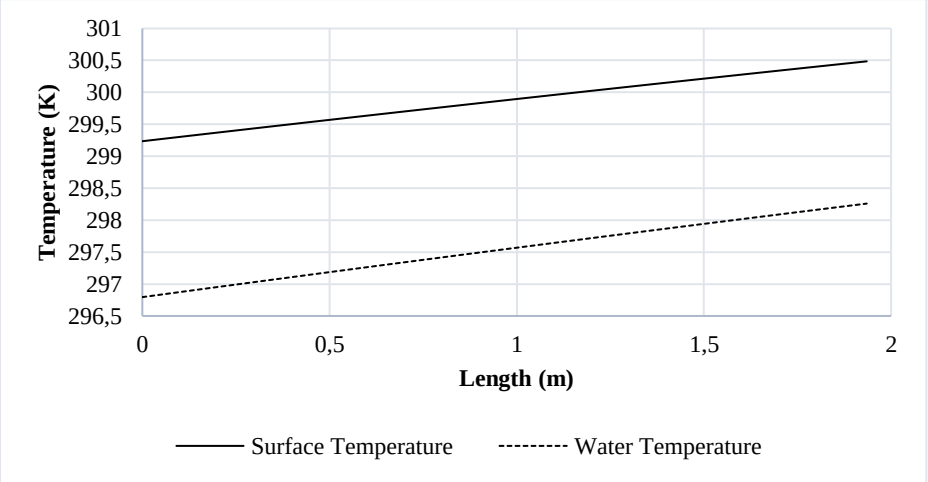

Figure 7. Temperature profile for the simulations.

3.4 Experimental Results

Looking forward a validation of the model, experimental results were needed to situate the accuracy level of the model. The Data was obtained by GREEN PUC Minas laboratory tests in diverse conditions, so it was possible to compare different situations.

Tables 4 and 5. Experimental Data and Model Data.

E. Data	T_n [°C]	T_∞ [°C]	$T_{f\,in}$[°C]	$T_{f\,out}$[°C]
Point 1	22,89	13,37	23,65	24,85
Point 2	24,59	14,54	24,50	25,83
Point 3	26,64	16,86	32,75	33,46
Point 4	27,20	17,19	33,13	33,82
Point 5	27,96	18,55	39,41	39,48
Point 6	28,92	19,16	45,64	45,23
Point 7	29,54	20,37	50,09	49,30

Model D.	$T_{f\,in}$[°C]	$T_{f\,out}$[°C]
Point 1	23,65	25,11
Point 2	24,50	25,98
Point 3	32,75	33,70
Point 4	33,13	34,10
Point 5	39,41	39,89
Point 6	45,64	45,64
Point 7	50,09	49,75

Table 6. Difference in output temperature.

Point	E. Data [°C]	Model D. [°C]	ΔT
Point 1	24,85	25,11	0,26
Point 2	25,83	25,98	0,15
Point 3	33,46	33,70	0,24
Point 4	33,82	34,10	0,27
Point 5	39,48	39,89	0,41
Point 6	45,23	45,64	0,41
Point 7	49,30	49,75	0,45
Average ΔT			***0,31***

Firstly, it is important to mention that for higher input temperatures like Points 6 and 7 the fluid output, as expected, lost more heat to the environment that held within it. That manly shows the cohesiveness of the model, it cannot only increase the temperature but also decrease it.

Secondly, it was possible to observe that the model values were always bigger than the experimental data, one reason for that is because the assumptions 3,4 and 8 combined. In (Silva, F.V.M.) the flow rate in each tube were different a possible explanation for that is the fact that the header also receives solar radiation, which implies in a gain of the fluid temperature along itself, considering the properties dependent of the temperature, the water density would get smaller, but it viscosity would get bigger, therefore it would be easier for the fluid to flow at the end of the header leading for a grater flow ate the tube on the end and a smaller flow on the beginning.

If the inlet temperature were the same for a variant flow in each tubes, Q_u for L = 0 would be the same, since the calculation of Q_u does not vary with the mass flow, but with Eq. (11) it says that for the tubes with smaller mass flows, $\dot{m}$, the gain of temperature by length unit is greater then for the tubes with grater mass flow. Due to this looking to the Eq. 10 T_s would be greater along the tube length, with Eq. (7) T_s and T_f increase, it still not possible to take any conclusions, but looking to the Eq.(5) and (6), the same T_s increases, but T_∞ and T_n stay the same, therefore, Q_{conv} and Q_{Rad} increase, analyzing Eq.(3), if Q_{conv} and Q_{Rad} increase Q_u must decrease and with the Eq.(13) to (15) it implies in a smaller efficiency and therefore the $T_{f\,out}$ of the model will always be bigger than the experimental data.

4. CONCLUSIONS

Observing the collector's behaviour on section 3.1, it is possible to see that it has a behaviour close to a logarithmic function, tending to a maximum value of T_f tending to T_s, and in the other hand, a linear behaviour close to a horizontal line on the section 3.3. These kinds of behaviour were expected for a solar collector in these conditions.

It is understood that the smaller the size of the element, the closer to reality will be the values of temperature difference, total heat absorbed, efficiency.

It is possible to observe that for n_e from the value 300 on, the variation of the results becomes negligible, that is, it spends more processing time to improve only a little the results. So, depending on the level of accuracy that is required, it is not necessary to use large values of n_e, since in the end the variation is minimal. It is possible to see that with higher mass flow rates, less elements are required.

It was clear that the experimental data obtained was close to the values simulated. Better results can be achieved by including the header in the simulation, varying the properties with temperature and considering the flow in each tube as variant.

5. ACKNOWLEDGEMENTS

This study was financed in part by the Coordenação de Aperfeiçoamento de Pessoal de Nível Superior - Brasil (CAPES) - Finance Code 001. The authors are also thankful to FAPEMIG, CNPq, and PUC Minas.

6. REFERENCES

Alghoul, M.A., Sulaiman, M.Y., Azmi, B.Z. and Wahab, M., 2005. “Review of materials for solar thermal collectors”. *Anti-Corrosion Methods and Materials*, Vol. 52, pp. 199-206.

Buena, M., Perers, B., Eicher, S., Hildbrand, C., Bony, J. and Citherlet, S., 2015. “Mathematical modelling of unglazed solar collectors under extreme operating conditions”. *Solar Energy*, Vol. 118, pp. 547-561. Elsevier Ltd. Retrieved from https://doi.org/10.1016/j.solener.2015.06.012

Buonomano, A., De Luca, G., Figaj, R.D. and Vanoli, L., 2015. “Dynamic simulation and thermo-economic analysis of a PhotoVoltaic/Thermal collector heating system for an indoor-outdoor swimming pool”. *Energy Conversion and Management*, Vol. 99, pp. 176-192. Elsevier Ltd. Retrieved from https://doi.org/10.1016/j.solener.2015.04.022

Cengel, Y.A., 2002. *Heat Transfer: A Practical Approach*. McGraw-Hill, New York, 2nd edition.

Cengel, Y.A., Cimbala, J.M., 2006. *Fluid Mechanics: Fundamentals and Applications*. McGraw-Hill, New York, 2nd edition.

Cunio, L.N. and Sproul, A.B., 2012. “Performance characterisation and energy savings of undercovered swimming pool solar collectors under reduced flow rate”. *Solar Energy*, Vol. 86, pp. 1511-1517. Elsevier Ltd. Retrieved from https://doi.org/10.1016/j.solener.2012.02.012

Duffie, J.A., and Beckman, W.A., 2013. *Solar Engineering of Thermal Processes*. John Wiley & Sons, New Jersey, 4th edition.

Evangelisti, L., Vollaro, R.D.L. and Asdrubali, F., 2019. “Latest advances on solar thermal collectors: A comprehensive review”. *Renewable and Sustainable Energy Reviews*, Vol. 114. Elsevier Ltd. Retrieved from https://doi.org/10.1016/j.rser.2019.109318

Gunjo, D.G., Mahanta, P. and Robi, P.S., 2017. "CFD and investigation of flat plate solar water heating system under steady state condition". *Renewable Energy*, Vol. 106, pp. 24-36. Elsevier Ltd. Retrieved from https://doi.org/10.1016/j.solener.2016.12.041

Helvaci, H.U. and Khan, Z.A., 2015. "Mathematical modelling and simulation of multiphase flow in a flat plate solar energy collector". *Energy Conversion and Management*, Vol. 106, pp. 139-150. Elsevier Ltd. Retrieved from https://dx.doi.org/10.1016/j.enconman.2015.09.028

Incropera, F.P., Bergman, T.L., Lavine, A.S. and Dewitt, D.P., 2010. *Fundamentals of heat and mass transfer*. John Wiley & Sons, New Jersey, 7th edition.

International Energy Agency., 2019. *Solar Heat Worldwide*. Weiss, W. and Spörk-Dür, M. Retrieved from https://www.iea-shc.org/Data/Sites/1/publications/Solar-Heat-Worldwide-2019.pdf

Missirlis, D., Martinopoulos, G., Tsilingiridis, G., Yakinthos, K. and Kyriakis, N., 2014. "Investigation of the heat transfer behaviour of a polymer solar collector for different manifold configurations". *Renewable Energy*, Vol. 68, pp. 715-723. Elsevier Ltd. Retrieved from https://doi.org/10.1016/j.solener.2014.02.008

Mitkiewicz Silva, F.V., Cardoso Diniz, A.S.A., Braga, D.S., Pataro Faria, L.P., Chaves Barbosa, E.M., Camatta Santana, V.A. and Maia, C.B., 2019. "Numerical analysis of unglazed solar pool collector". In *Proceedings of the 22nd International Congress of Mechanical Engineering - COBEM 2019*. Uberlândia, Brazil.

Morrison, G.L., Gilliaert, D., 1992. "Unglazed Solar Collector Performance Characteristics". *Journal of Solar Engineering*, Vol. 114, pp. 194-199.

Patti, A. and Acierno, D., 2019. "Polypropylene - Polymerization and Characterization of Mechanical and Thermal Properties". *Thermal Conductivity of Polypropylene-Based Materials*. IntechOpen Retrieved from http://dx.doi.org/10.5772/intechopen.84477

Reiter, C., Brandmayr, S., Trinkl, C., Zörner, W. and Hanby, V.I., 2013. "Performance optimisation of polymeric collectors by means of dynamic simulation and sensitivity analysis". *Energy Procedia*, Vol. 48, pp. 181-191.

Sharples, S. and Charlesworth, P.S., 1998. "Full-Scale Measurements Of Wind-Induced Convective Heat Transfer From A Roof-Mounted Flat Plate Solar Collector". *Solar Energy*, Vol. 62, pp. 69-77.

Test, F.L., Lessman, R.C., Johary, A., 1981. "Heat transfer during wind flow over rectangular bodies in the natural enviroment". *ASME Journal, Heat Transfer 103.*

7. RESPONSIBILITY NOTICE

The authors are the only responsible for the printed material included in this paper.